

Tribological and corrosion properties of plasma nitrided and nitrocarburized 42CrMo4 steel

D Kusmic¹ and D Van Thanh²

^{1,2} Department of Mechanical Engineering, Faculty of Military Technology,
University of Defence, Kounicova 65, 662 10 Brno, Czech Republic, EU

E-mail: ¹david.kusmic@unob.cz, ²thanhvan.doan@unob.cz

Abstract. This article deals with tribological and corrosion resistance comparison of plasma nitrided and nitrocarburized 42CrMo4 steel used for breech mechanism in the armament production. Increasing of materials demands (like wear resistance, surface hardness, running-in properties and corrosion resistance) used for armament production and in other industrial application leads in the field of surface treatment. Experimental steel samples were plasma nitrided under different nitriding gas ratio at 500 °C for 15h and nitrocarburized for 45 min at temperature 590°C and consequently post-oxidized for 10 min at 430°C. Individual 42CrMo4 steel samples were subsequently metallographically evaluated and characterized by hardness and microhardness measuring. The wear test “ball on disc” was realized for measuring of adhesive wear and coefficient of friction during unlubricated sliding. NSS corrosion tests were realized for corrosion resistance evaluation and expressed by corroded area and calculated corrosion rate. The corrosion resistance evaluation is by the surface corrosion-free surfaces evaluation supplemented using the laser confocal microscopy. Due to different surface treatment and plasma nitriding conditions, there are wear resistance and corrosion resistance differences evident between the plasma nitrided steel samples as well.

1 Introduction

Plasma nitriding is a chemical-heat treatment process that is widely used for increase of surface hardness, fatigue strength, corrosion resistance and to improve tribological behavior mostly of steels [1]. The treatment temperature of plasma nitriding process is usually set below the eutectoid temperature in Fe-N diagram (590 °C). It is suitable to set the nitriding temperature below the last heat-treatment procedure temperature, to ensure unchanged microstructure of the core of prior heat-treatment (e.g. tempered structure). Thanks to diffusion of nascent nitrogen (during the nitriding process generated) a compound and diffusion layer is created. Compound (white) layer mostly consists of the ϵ -Fe₂₋₃N and γ' -Fe₄N iron nitrides, as well as of mixture of alloying elements nitrides like Al, Cr, Mo, V [2-4]. This surface compound layer is characterized by increased hardness and good corrosion resistance. Increased corrosion resistance can be additionally increased by post-oxidation process, applied directly after plasma nitriding process in the device [5, 6]. The formed oxide layer is able to cover the micropores and improves the corrosion resistance of nitrided steel [7-10].

This paper is focused on evaluation of wear and corrosion resistance of plasma nitrided and nitrocarburized 42CrMo4 (AISI 4137/4140) steel and compared to tempered one. Plasma nitriding process was applied under different nitriding gas ratio (H₂:N₂) for 15 h. The wear tests “pin on disc” were employed to find out the adhesive wear and coefficient of friction during unlubricated sliding (dry sliding). The corrosion resistance was tested using the NSS corrosion test according with ISO



9227 standard, visually and gravimetric evaluated. After removing the corrosion products, the surfaces were evaluated using the laser confocal microscopy. Results of wear and corrosion tests were further supplemented by metallographic documentation and measuring of tie-layer thickness. Thickness and microhardness of created layers were measured by Vickers microhardness method in accordance with DIN 50190 standard.

2 Experimental

For this study was used 42CrMo4 (AISI 4137/4140) steel with the following chemical composition (in wt.%): 0.40 C, 1.08 Cr, 0.63 Mn, 0.27 Si, 0.15 Mo, 0.10 Ni, 0.0019 S, 0.0012 P. Chemical composition was verified using the Q4 Tasman device, calibrated by the Fe 130 and Fe 140 standards. Experimental samples were heated at 850 °C for 20 min, oil quenched, tempered at 550°C for 40 min for microstructure homogenization and to achieve standard mechanical properties. All the surfaces of samples were grinded and cleaned in ethanol prior plasma nitriding and nitrocarburizing (known as Tenifer®).

Plasma nitriding was performed under two nitriding gas ratio in the RUBIG PN 60/60 device (marked as PN1 and PN2), for plasma nitriding conditions see table 1. Tenifer® (marked as NC) essentially is a technology including nitrocarburizing process in salt bath of SURSULF solution for 45 min under temperature of 590 °C followed by oxidation process in salt bath of OXINIT solution for 10 min at 430 °C for corrosion-resistant oxides Fe₃O₄ (magnetite) and Fe₂O₃ (hematite) creation (marked as NC).

Table 1. Plasma nitriding process conditions.

Process	Temperature (°C)	Duration (h)	Pressure (Pa)	Bias (V)	Gas flow (<i>l.h⁻¹</i>)	
					H ₂	N ₂
Plasma cleaning	480	0.5	80	800	20	2
PN1- 3H₂:1N₂	500	15	280	530	24	8
PN2- 1H₂:3N₂	500	15	280	530	8	24

Thickness of diffusion layer was evaluated by microhardness testing in accordance with DIN 50190 standard using the automatic microhardness tester LECO LM 247 AT equipped with the AMH43 software allowed to investigate diffusion layer depth in direction from surface to the core at 50 g load and 10 s dwell. The final microhardness profile and measuring of diffusion layer depth was determined by 18 indentations with variable indentation spacing. The compound and diffusion layer characteristics are summarized in table 2.

Table 2. The thickness of compound layer and layer case depth.

	Case depth (μm)	Thickness of compound layer (μm)	Thickness of oxide layer (μm)	Microhardness (HV0.05)
Tempered	-	-	-	366
PN 1 - 3H₂:1N₂	200	3.6	-	681
PN 2 - 1H₂:3N₂	240	7.4	-	778
NC	120	16.5	1	772

For metallographic testing, all samples were crosswise cutted, wet grinded using silicon carbide paper with grit size from 80 to 2000, subsequently polished and finally etched by Nital. The cross-structure documentation and compound layer thickness measuring was realized using the opto-digital microscope OLYMPUS DSX 500. The bainitic–sorbite microstructure of tempered sample and structure of nitrided and nitrocarburized layers can be seen in figure 1.

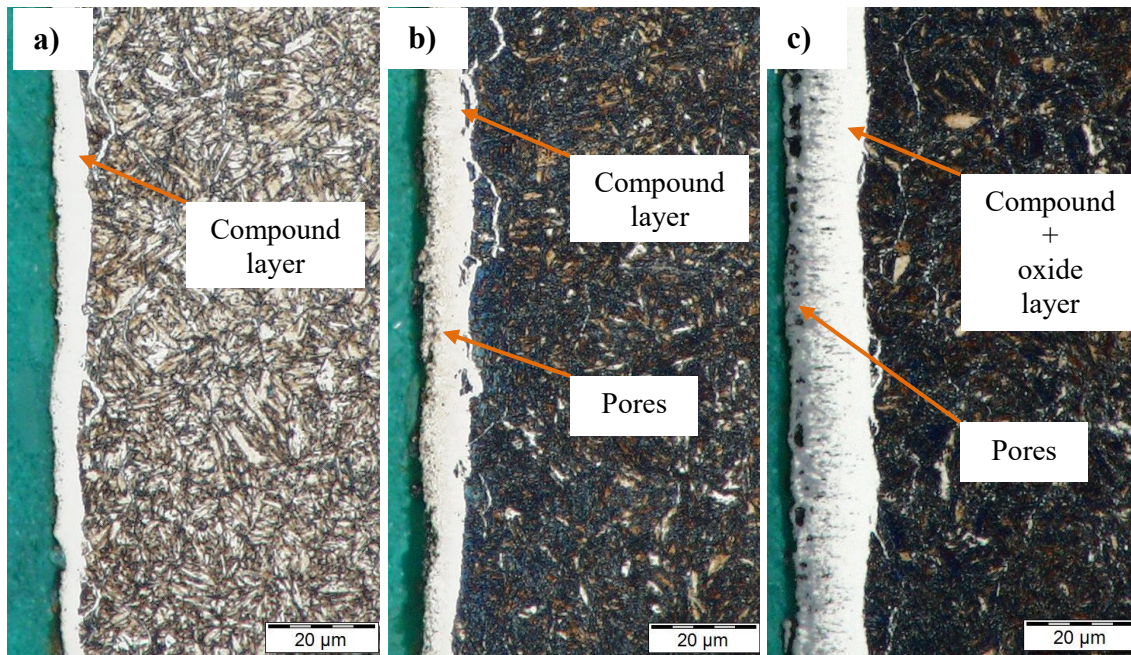


Figure 1. Cross-sectional microstructures (a) PN1 (3H₂:1N₂, 15h), (b) PN2 (1H₂:3N₂, 15h) and (c) NC (nitrocarburized).

It can be clearly seen that the case depth (see table 2.) and thickness of compound layer increases with N₂ ratio in nitriding gas mixture from 5.4 μm as seen in Figure 1(a) for PN1 sample to 8.6 μm in Figure 1(b) for PN2 sample gas mixture. Increased N₂ ratio in nitriding gas mixture has a significant influence to compound layer porosity, which increases with compound layer thickness, can be seen in figure 1(b). Increased porosity of compound layer (reached 16.5 μm), can be seen in figure 1(c) of nitrocarburized steel. Generally better corrosion resistance of plasma nitrided steel under 1H₂:3N₂ nitriding gas mixture (formed predominantly by ε-Fe₂₋₃N nitride) can be affected. Increased porosity of compound layer can cause reduction of corrosion resistance and delamination of stressed compound layer. Contrariwise significant improving of corrosion resistance of nitrocarburized steel can be expected, due to post-oxidation process. Thanks to post-oxidation process covering of pores by 1 μm thick oxide layer (dominantly formed by Fe₃O₄ oxides) can heal the surface, see figure 1. (c) [10].

3 Results and discussions

3.1 Wear tests

The wear tests “ball on disc” in accordance with ASTM G99-95 standard were performed using the CETR UMT-3 tribometer, for coefficient of friction and in combination with the Talysurf CLI 1000 profilometer to evaluate the wear track for wear rate calculation:

$$W = \frac{V}{F \cdot s} (m^3 \cdot N^{-1} \cdot m^{-1}) \quad (1)$$

where W is the wear per unit load per sliding distance, V (m³) is the worn volume, F (N) is the applied load and s (m) is the sliding distance. The measurement of wear trace profile was realized using the Talysurf CLI 1000 profilometer. Four measurements of canopy profiles were used for calculating the worn volume (see figure 2):

$$V = S \cdot \Pi \cdot 2r (m^3) \quad (2)$$

where the S is the average canopy area (m^2) and r the radius of wear test measurement (m).

For wear tests was used the carbide wolfram ball of diameter 6.3 mm with hardness of 92 HRA. The tests parameters were set up as following: applied load of 20 N, rotary velocity of 500 rpm and 13500 cycles.

The friction coefficient is a dimensionless quantity, defined as quotient of normal and friction force. Hence, this value changes continually with surface state, duration and environment [11].

The dependence of friction coefficient vs. time of treated steel samples – carbide wolfram contact is plotted in figure 3.

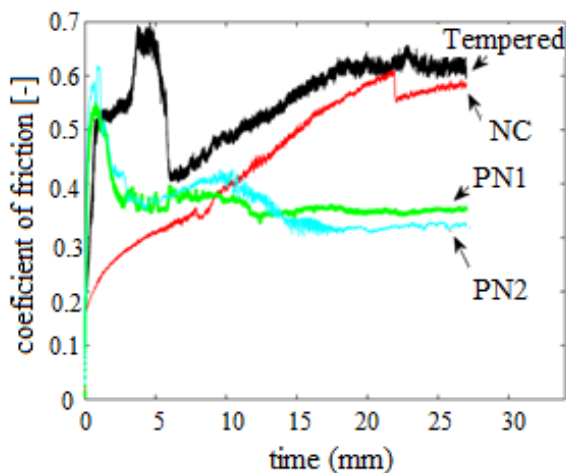


Figure 3. Coefficient of friction.

The tempered steel sample shows the highest value of friction coefficient ($\mu = 0.62$). The nitrocarburized (NC) sample indicated the second greatest coefficient of friction ($\mu = 0.58$).

The nitrided samples showed the lowest value of friction coefficient and it is very stable. The sample PN2 (1H₂:3N₂) provides the lowest coefficient ($\mu = 0.32$) and sample PN1 ($\mu = 0.35$).

The coefficient of friction of nitrocarburized steel samples gradient is not as steep as others at to beginning of measurement, but after 20 min of measuring reached high stable value of coefficient of friction. The coefficient of friction μ was considered as an average value of stable section. In this article experiment, the wear rate is not proportional to the values of friction coefficient.

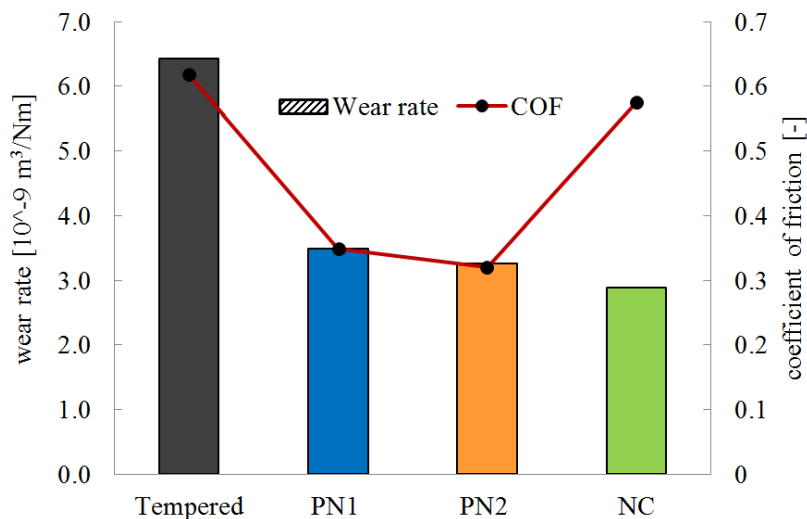


Figure 4. Tribological characters.

The interrelationship between coefficient of friction and calculated wear rate, as in equation (1), are summarized in figure 4. The tempered steel sample shows the highest wear rate and friction coefficient. Although nitrocarburizing enhances the value of $\mu = 0.58$ but wear rate of this sample is the lowest. Sample PN2 exhibits very positive results, that both two values of coefficient of friction and wear rate are very low (see figure 4).

3.2 Corrosion behaviour

The tempered, plasma nitrided and nitrocarburized samples were exposed to a 5 % neutral sodium chloride solution (NSS) fog in accordance with ISO 9227 standard in the VLM GmbH SAL 400-FL corrosion chamber under following conditions: the temperature of 35 ± 2 °C, 5 % neutral sodium chloride solution, the amount of vapor condensation was set for $1 \div 2$ ml.h⁻¹ on square of 80 cm², pH $6.5 \div 7.2$, the suspension angle of 20° from the vertical line, after every exposition period (2, 4, 8, 24, 48, 72, 96, 144 and 196 hours) were the exposed samples documented (see figure 5). The samples were degreased before the corrosion testing by the ethylalcohol.

The corrosion resistance was during the evaluation periods after drying documented and visually evaluated using the QuickPHOTO Industrial 2.3 software with Phase analyses application, as seen in figure 5.

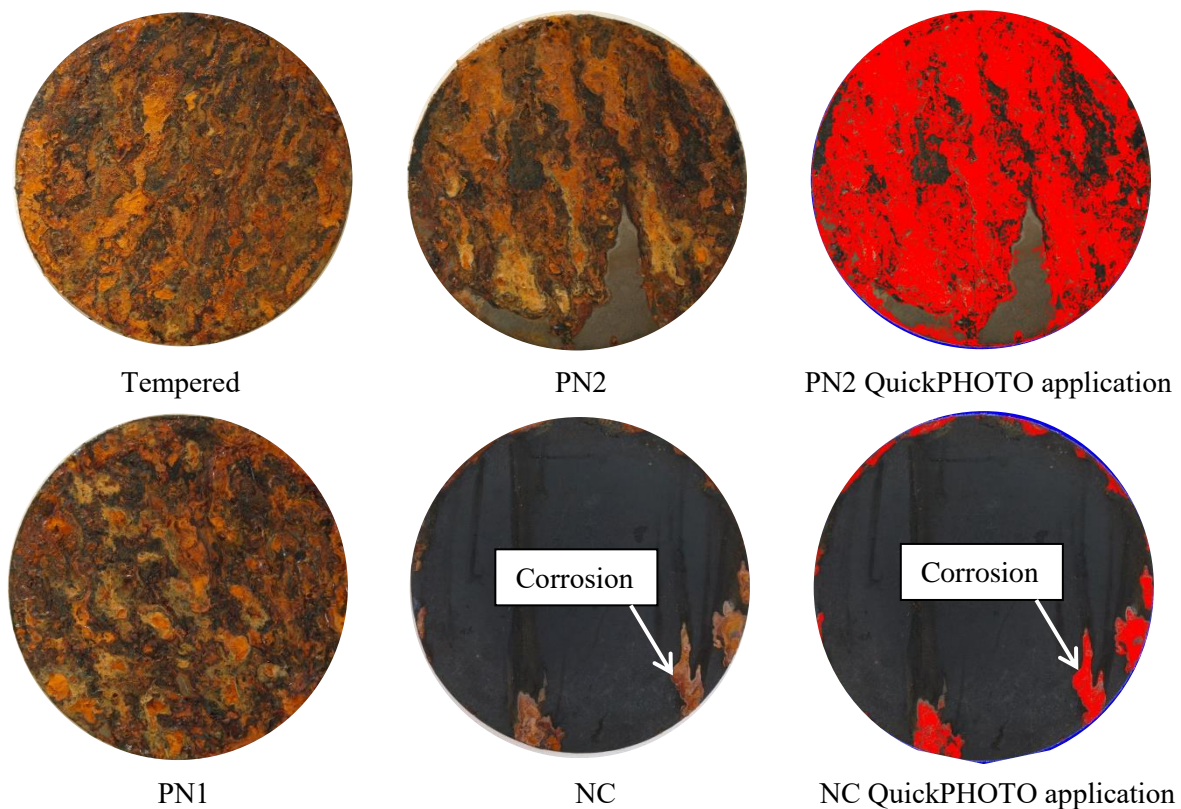


Figure 5. Visual evaluation after 72h in NSS.

Uniform type of corrosion attack of tempered steel sample was expected and combined corrosion attack or pitting of plasma nitrided and nitrocarburized and subsequently post-oxidized steel samples. The best results achieved the nitrocarburized and subsequently post-oxidized steel samples. Good corrosion resistance can be attributed to Fe₃O₄ and Fe₂O₃ oxides. Oxide layer formed during the post-oxidizing process, covers the micropores in the compound layer and ensure passivity [12]. Increased corrosion resistance comparing to tempered sample was confirmed for PN1 and PN2 samples, it is evident that the thickness and compactness of compound layer plays a role (see figure 1, table 2). The corrosion progress of corroded surface area vs. exposure period is plotted in figure 6. During the corrosion tests the weight gain was measured and the corrosion rate was calculated:

$$K_{corr} = \frac{m_t}{S.t} \left(mg.cm^{-2}.h^{-1} \right) \quad (3)$$

where the m_t (mg) is weight gain in evaluated time period defined by $m_t = m_h - m_{int}$ (mg), the m_h (mg) is the measured weight in evaluated time period and m_{int} (mg) is the initial weight before corrosion test, S (cm²) is the total surface area and t (h) is the evaluated time period.

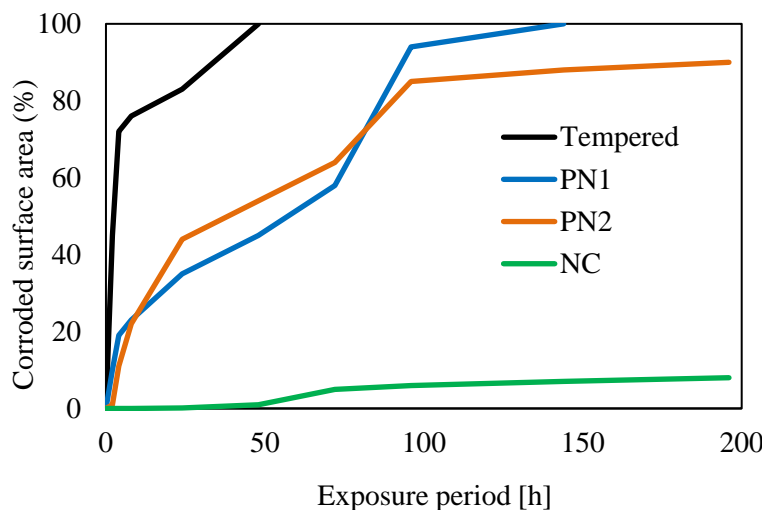


Figure 6. Corroded surface area vs. exposure (NSS).

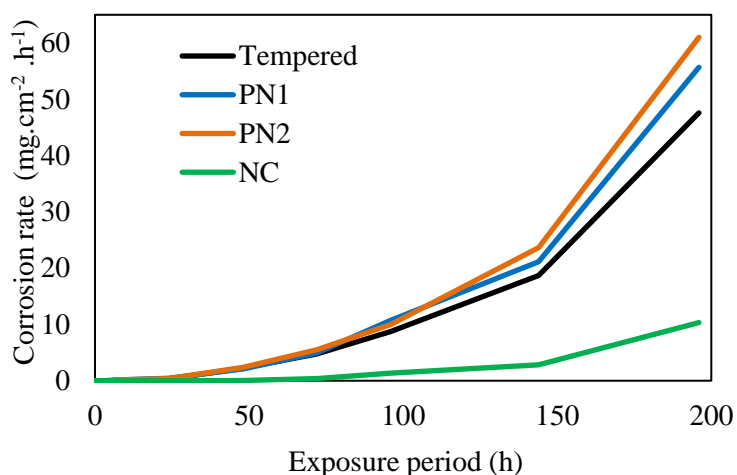


Figure 7. Corrosion rate - weight gain (NSS).

accordance with CSN ISO 11463: 1997 (identical to ISO 11463: 1995 standard):

$$PF = \frac{\text{deepest penetration}}{\text{average penetration}} (-) \quad (4)$$

if the pitting factor (PF) is equal to value 1, then represents uniform corrosion. Higher value of pitting factor represents deeper pits penetration. Values of PF were set as following: 1 (tempered sample), 1.34 (PN1), 1.22 (PN2) and 1.24 (NC). Corrosion attack of plasma nitrided 42CrMo4 steel is a combined one, a combination of general and pitting corrosion with increased pitting penetration. Increased pitting penetration is in this case on compound layer compactness and porosity dependent (see figure 1 b).

Corrosion rates of all tested samples are plotted in figure 7. It is evident that the trend of corroded surface area progress (figure 6) is not same as the corrosion rate progress (figure 7). It was necessary to investigate the corrosion mechanism of plasma nitrided samples PN1 and PN2, why is the corrosion rate of sample PN1 and PN2 higher than of tempered sample.

For corrosion mechanism investigation were all corroded surfaces in accordance with ISO 8407 standard chemically and mechanically cleaned. For this purpose was used the solution of 500 ml of HCl, 3.5 ml of urotropin and 496.5 ml of H₂O and afterwards the topography was by the laser confocal microscopy (Olympus OLS 3000) studied (see figure 8) and the pits could be measured. Thanks to laser confocal microscopy was the type of corrosion attack clear. Tempered sample was corroded by uniform corrosion sample PN1 and PN2 by mixed corrosion attack (uniform and pitting corrosion) and NC sample dominantly by pitting. The depth of pitting could be by pitting corrosion factor expressed in

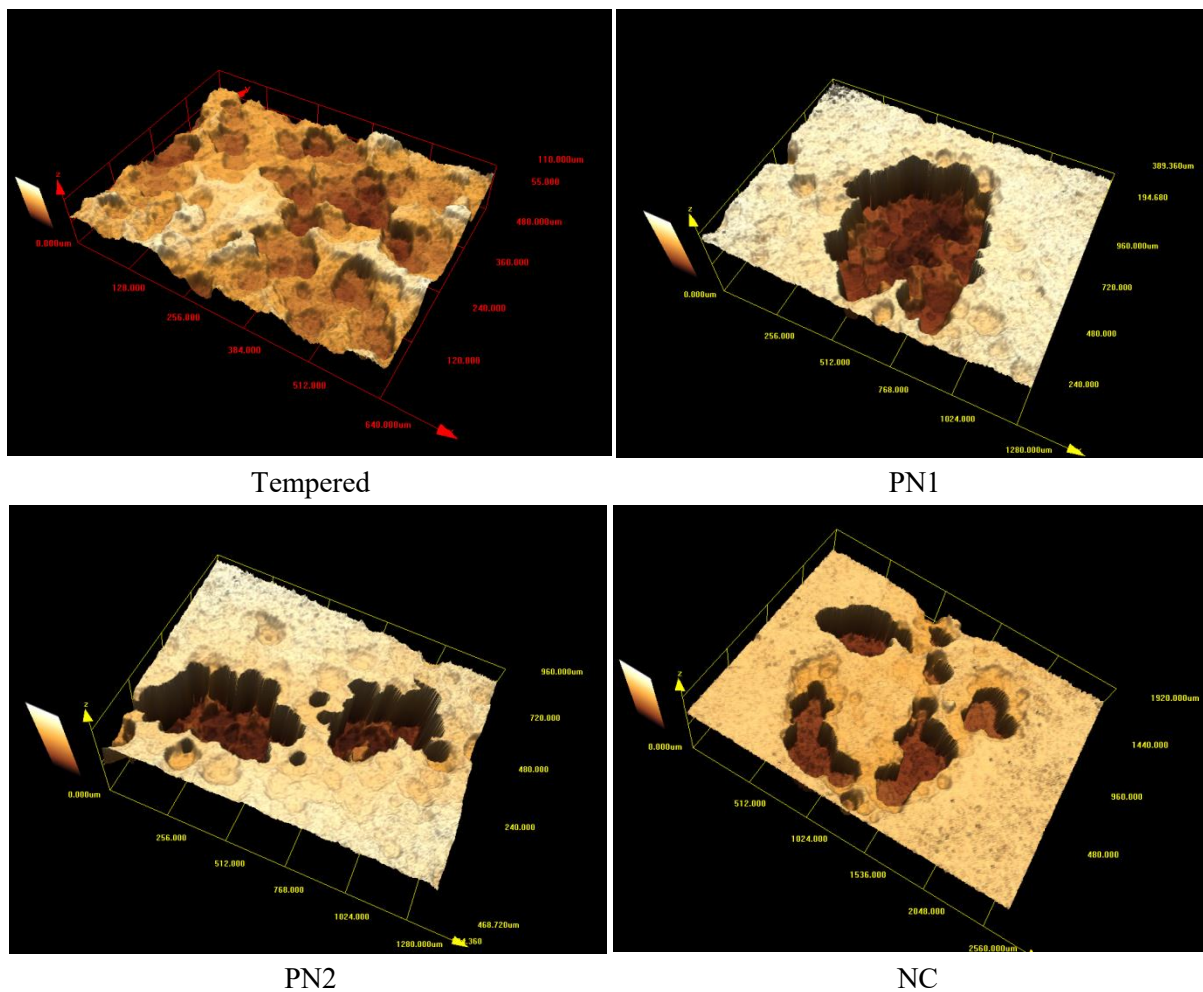


Figure 8. 3D surface evaluation (Olympus OLS 3000).

4 Conclusions

42CrMo4 steel samples were prepared for wear and corrosion resistance evaluation. Tempered steel samples were compared to plasma nitrided for 15 h in different nitriding gas ratio ($3\text{H}_2:1\text{N}_2$ for PN1 and $1\text{H}_2:3\text{N}_2$ for PN2) and to Tenifer® technology (NC - nitrocarburizing followed by post-oxidation process).

Using the reverse ratio nitriding atmosphere has a positive influence to wear resistance and to value of coefficient of friction (see figure 4). Increased wear resistance of PN2 sample could be attributed to increased hardness, thickness and phase composition of compound layer (increased ratio of $\text{Fe}_2\text{-}_3\text{N}$). Increased porosity of compound layer was found of the PN2 ($1\text{H}_2:3\text{N}_2$) and NC samples. This porosity negatively influences the corrosion resistance of plasma nitrided steel. Increased pitting and general corrosion was evident. This combination of corrosion attack negatively influences the corrosion rate (weight gain). The visual evaluation of corrosion resistance was found as biased and therefore a combination of visual and gravimetric evaluation was used.

Best corrosion resistance reached Tenifer® thanks to $1\mu\text{m}$ thin compact Fe_3O_4 oxide layer covering the surface pores. This surface layer is especially resistant to abrasion, corrosion and galling.

Acknowledgements

The paper has been prepared thanks to the support of the project *The Development of Technologies, Design of Firearms, Ammunition, Instrumentation, Engineering of Materials and Military Infrastructure "VÝZBROJ (DZRO K201)." and "Surface technology in applications special techniques SV16-216."*

References

- [1] Maniee A. Mahboubi F and Soleimani R 2014 The study of tribological and corrosion behavior of plasma nitride 34CrNiMo6 steel under hot and cold wall conditions *Journal Materials and Design*. vol. 60 2014
- [2] Pokorný Z. Hruby V and Studeny Z 2016 Effect of nitrogen on surface of layers *Journal Metallic Materials*. vol. 54 no. 2 2016
- [3] Pye D 2003 Practical nitriding and ferritic nitrocarburizing ed ASM International (Materials Park: Ohio) chapter 4 pp 31–35
- [4] Nikolussi M. Leinweber A et al. 2007 Examination of phase transformations in the system Fe-N-C by means of nitrocarburising reactions and secondary annealing experiments, the $\alpha+\epsilon$ two-phase equilibrium *Journal Material Research*. vol. 98 no.11 pp 1086-92
- [5] Dong-Cherng W 2009 Plasma nitriding of plastic mold steel to increase wear and corrosion properties *Journal Surface&Coatings Technology*. vol. 204 pp 511-19
- [6] Yang L. Liang W. Dandan Z and Lie Shen 2010 Improvement of corrosion resistance of nitrided low alloy steel by plasma post-oxidation *Journal Applied Surface Science*. vol. 256 Issue 13 pp 4149-52
- [7] Basu A. MAJUMDAR J D et al. 2008 Corrosion resistance improvement of high carbon low alloy steel by plasma nitriding *Journal Materials Letters*. vol. 62 pp 3117–20
- [8] Kusmic D and Dobrocky D 2015 Corrosion Resistance of Plasma Nitrided Structural Steels *Journal Manufacturing Technology*. vol. 15 no. 1 pp 64-69
- [9] Ebrahimi M. Heydarzadeh Sohi M et al. 2010 Effect of plasma nitriding temperature on the corrosion behavior of AISI 4140 steel before and after oxidation *Journal Surface & Coatings Technology*. vol. 205 pp 261-66
- [10] Marusic K. Otmacic H et al. 2006 Modification of carbon steel surface by the Tenifer® process of nitrocarburizing and post-oxidation *Journal Surface & Coatings Technology*. vol. 201 pp 3415-21
- [11] Wu J. Liu H et al. 2015 Enhancement of corrosion resistance for plasma nitride AISI 4110 steel by plain air plasma post-oxidizing *Journal of Alloys and Compounds*. vol. 632 pp. 397-01